5

Rock Mass Hydraulic Conductivity Estimated by Two Empirical Models

Shih-Meng Hsu[1], Hung-Chieh Lo[1], Shue-Yeong Chi[1] and Cheng-Yu Ku[2]
[1]Sinotech Engineering Consultants, Inc.
[2]National Taiwan Ocean University,
Taiwan

1. Introduction

Undertaking engineering tasks such as tunnel construction, dam construction, mine development, the abstraction of petroleum, and slope stabilization require the estimation of hydraulic conductivity for fractured rock mass. The understanding of hydraulic properties of fractured rock mass, which involves the fluid flow behaviour in fractured consolidated media, is a critical step in support of these tasks. To obtain hydraulic properties of fractured rock mass, double packer systems can be adopted (NRC 1996). They can be used to determine the hydraulic conductivity in a portion of borehole using two inflatable packers. Although this type of test can directly measure the hydraulic parameter, costs of the testing are fairly high. Several studies (Snow, 1970; Louis, 1974; Carlsson & Olsson, 1977; Burgess, 1977; Black, 1987; Wei et al., 1995;) have proposed the estimation of rock mass hydraulic conductivity using different empirical equations, which were based on the concept that rock mass permeability decreases with depth, as shown in Table 1. These empirical equations provide a great feature for characterizing rock mass hydraulic properties quickly and easily. However, the applicability of these equations is very limited because depth is not the only significant variable on the prediction of rock mass permeability. Hydraulic properties of rock mass may vary with geostatic stress, lithology and fracture properties, including fracture aperture and frequency, fracture length, fracture orientation and angle, fracture interconnectivity, filling materials, and fracture plane features (Lee & Farmer, 1993; Sahimi, 1995; Foyo et al., 2005; Hamm et al., 2007). Thus, a more applicable empirical equation for estimating hydraulic conductivity of rock mass possibly must include the aforementioned factors.

This chapter proposes two empirical models to estimate hydraulic conductivity of fractured rock mass. The first empirical model was based on the rock mass classification concept. The study developed a new rock mass classification scheme for estimating hydraulic conductivity of fractured rocks. The new rock mass classification system called as "HC-system" based on the following four parameters: rock quality designation (RQD), depth index (DI), gouge content designation (GCD), and lithology permeability index (LPI). HC-values can be calculated from borehole image data and rock core data. The second empirical model was simply based on results of borehole televiewer logging, flowmeter logging and packer hydraulic tests. Three borehole prospecting techniques for fractured rock mass hydrogeologic investigation were performed to explore various hydrogeologic characteristics, such as fracture width, fracture angle, flow velocity and hydraulic

Equation	Reference
$k = \alpha z^{-b}$	Black (1987) a and b are constants. z is the vertical depth below the groundwater surface.
$\log K = -8.9 - 1.671 \log Z$	Snow (1970) K (ft^2) is the permeability. z (ft) is the depth.
$K = 10^{-(1.6 \log z + 4)}$	Carlson and Olsson (1977) K (m/s) is the hydraulic conductivity. z (m) is the depth.
$K = K_s e^{(-Ah)}$	Louis (1974) K (m/s) is the hydraulic conductivity. K_s is the hydraulic conductivity near ground surface. H (m) is the depth. A is the hydraulic gradient.
$\log K = 5.57 + 0.352 \log Z$ $-0.978(\log Z)^2 + 0.167(\log Z)^3$	Burgess (1977) K (m/s) is the hydraulic conductivity. Z (m) is the depth.
$K = K_i[1 - Z / (58.0 + 1.02Z)]^3$	Wei et al. (1995) Z is the depth. K is the hydraulic conductivity. K_i (m/s) is the hydraulic conductivity near ground surface.

Table 1. Diverse approximations for estimating rock mass hydraulic conductivity

conductivity. By adopting a correlation analysis, the dependence between hydraulic conductivity and other prospecting data can be identified. The consequence results can be used to determine rock mass hydraulic conductivity.

2. The first empirical model

The classical rock mass classification systems have gained wide attention and are frequently used as powerful design aids in rock engineering. A great feature of the existing systems is that the characterization of rock mass properties for specific engineering purposes can be quickly obtained at a relatively low cost. There are six common systems used for engineering purposes, including Rock load (Terzaghi, 1946), Stand-up time (Lauffer, 1958), RQD (Deere et al., 1967), RSR (Wickham et al., 1972), RMR (Bieniawski, 1973), and Q-system (Barton et al., 1974). The above systems or other available systems were designed on the geomechanical assessment of rock mass. However, there is very limited study on rock mass permeability assessments (Bieniawski, 1989). Because permeability of rock mass is related to groundwater seepage into excavations for tunnels, mines, and other construction sites, Gates (1997) proposed the hydro-potential (HP) value as a new rock mass classification, semi-quantitative technique employed to evaluate the potential for developing groundwater in bedrock. The HP-value technique is a modification of the engineering rock mass quality designation (Q) originally developed for evaluation of rock competency in tunnel design and seismic rock fall susceptibility.

To reduce the cost of estimating the hydraulic parameter, the objective of the study presented herein is to propose a new application of the rock mass classification concept on

the estimation of hydraulic conductivity of fractured rocks. The new rock mass classification system will be verified by in situ hydraulic test data from two hydrogeological investigation programs in three boreholes to demonstrate its rationality in predication of hydraulic conductivity of fractured rocks. Besides, the model verification using another borehole data with four additional in-situ hydraulic tests from similar geologic rocks was also conducted to further verify the feasibility of the proposed empirical HC model.

2.1 Components of new rock mass classification system

Prior to describing the new rock mass classification system, potential factors, including rock quality designation (RQD), depth index (DI), gouge content designation (GCD), and lithology permeability index (LPI), that may affect the degree of permeability should be considered. In addition, the rating approach for each factor that represents the magnitude of permeability is also described as follows.

2.1.1 Rock Quality Designation (RQD)

In rock engineering, from the mechanical point of view, the degree of fracturing stands for rock quality. This provides a simple index to judge the engineering quality of the rock. From the hydrogeological point of view, fractures reflect the ability of a formation to transmit water through fractures themselves. Thus, the degree of fracturing may be regarded as a factor in evaluating rock mass permeability.

To assess the influence of the fracture characteristic on permeability, the rock quality designation (RQD) index, which was developed by Deere et al. (1967), can be adopted. The RQD index was introduced over 40 years ago as an indicator of rock mass conditions. The RQD value is defined as the cumulative length of core pieces longer than 100 mm in a run (R_S) divided by the total length of the core run (R_T) and can be obtained from the following equation.

$$RQD = \frac{\sum Length\ of\ Intact\ and\ Sound\ Core\ Pieces\ >\ 100\ mm}{Total\ Length\ of\ Core\ Run,\ mm} \times 100\% = \frac{R_s}{R_T} \times 100\% \tag{1}$$

In this study, a core run for calculating a RQD value is herein defined as a selected zone of a hydraulic test. Equation (1) may be utilized to identify rock mass permeability.

2.1.2 Depth Index (DI)

Many researchers (for example Lee & Farmer, 1993; Singhal & Gupta, 1999) pointed out that rock mass permeability may decrease systematically with depth. The decrease in permeability with depth in fractured rocks is usually attributed to reduction in fracture aperture and fracture spacing. The reduction is due to the effect of geostatic stresses, and thereby the permeability of fractured rocks will reduce. The depth may be considered as a factor in evaluating rock mass permeability.

To assess the influence of the depth on permeability, a depth index called as DI was defined as the following equation.

$$DI = 1 - \frac{L_c}{L_T} \tag{2}$$

in which L_T is the total length of a borehole; L_c is a depth which is located at the middle of a double packer test interval in the borehole. The value of DI is always greater than zero and less than one. The greater the DI value, the higher the permeability.

2.1.3 Gouge Content Designation (GCD)

In general, the permeability of clay-rich gouges has extremely low values (Singhal & Gupta, 1999). The RQD value may decrease by an increase of fractures in a core run. If the fractures contain infillings such as gouges, permeability of the fractures will reduce. To assess the influence of the gouge materials on permeability, a gouge content designation index called as GCD was defined as the following equation.

$$GCD = \frac{R_G}{R_T - R_S} \tag{3}$$

in which R_G is the total length of gouge content. The value of GCD is always greater than zero and less than one. The greater GCD value stands for the more gouge content in a core run, and thereby it will reduce the permeability of the core run.

2.1.4 Lithology Permeability Index (LPI)

Lithology is the individual character of a rock in terms of mineral composition, grain size, texture, color, and so forth. For an intact rock, the magnitude of permeability depends largely on the individual character of the rock. It may be affected by the average size of the pores, which in turn is related to the distribution of particle sizes and particle shape. In sedimentary formations grain-size characteristics are most important because coarse-grained and well-sorted material will have high permeability as compared with fine-grained sediments like silt and clay. Thus, the lithology may be regarded as a factor in evaluating rock mass permeability.

To assess the influence of lithology on permeability, a lithology permeability index called as LPI was defined as Table 2.

2.2 Rock mass permeability system

As stated in Section 2.1, the rock mass permeability may be dependent on the following four parameters: rock quality designation (RQD), depth index (DI), gouge content designation (GCD), and lithology permeability index (LPI). However, the permeability is not simply affected by only one factor. It is possibly affected by any two factors, three factors or even all four factors. Thus, a rock mass classification scheme was applied to establish the rock mass permeability system. The new rock mass classification scheme is the product of the four parameters. It can account for the synthetic effect from the four parameters on permeability. The new rock mass classification system called as "HC-system" can be given by the following equation:

$$HC = \left(1 - \frac{RQD}{100}\right)(DI)(1 - GCD)(LPI) \tag{4}$$

The value of each parenthesis at the right hand side of Equation (4) is always greater than zero and less than one depending on the values assigned to the four parameters. The greater the value of each parenthesis, the higher the permeability. Thus, the system performs a

Lithology	Hydraulic conductivity (m/s)				Range of rating	Suggested Rating
	Reference[1]	Reference[2]	Reference[3]	$K_{average}$		
Sandstone	10^{-6}~10^{-9}	10^{-7}~10^{-9}	10^{-7}~10^{-9}	$10^{-7.5}$	0.8-1.0	1.00
Silty Sandstone	-	-	-	-	0.9-1.0	0.95
Argillaceous Sandstone	-	-	-	-	0.8-0.9	0.85
S.S. interbedded with some Sh.	-	-	-	-	0.7-0.8	0.75
Alternations of S.S & Sh.	-	-	-	-	0.6-0.7	0.65
Sh. interbedded with some S.S.	-	-	-	-	0.5-0.7	0.60
Alternations of S.S & Mudstone	-	-	-	-	0.5-0.6	0.55
Dolomite	10^{-6}~$10^{-10.5}$	10^{-7}~$10^{-10.5}$	10^{-9}~10^{-10}	10^{-8}	0.6-0.8	0.70
Limestone	10^{-6}~$10^{-10.5}$	10^{-7}~10^{-9}	10^{-9}~10^{-10}	10^{-8}	0.6-0.8	0.70
Shale	10^{-10}~10^{-12}	10^{-10}~10^{-13}	-	$10^{-10.5}$	0.4-0.6	0.50
Sandy Shale	-	-	-	-	0.5-0.6	0.60
Siltstone	10^{-10}~10^{-12}	-	-	10^{-11}	0.2-0.4	0.30
Sandy Siltstone	-	-	-	-	0.3-0.4	0.40
Argillaceous Siltstone	-	-	-	-	0.2-0.3	0.20
Claystone	-	10^{-9}~10^{-13}	-	10^{-11}	0.2-0.4	0.30
Mudstone	-	-	-	-	0.2-0.4	0.20
Sandy Mudstone	-	-	-	-	0.3-0.4	0.40
Silty Mudstone	-	-	-	-	0.2-0.3	0.30
Granite	-	-	10^{-11}~10^{-12}	$10^{-11.5}$	0.1-0.2	0.15
Basalt	10^{-6}~$10^{-10.5}$	10^{-10}~10^{-13}	-	$10^{-11.5}$	0.1-0.2	0.15

[1]B.B.S. Singhal & R.P. Gupta (1999)

[2]Karlheinz Spitz & Joanna Moreno (1996)

[3]Bear(1972)

Table 2. Description and ratings for lithology permeability index

numerical assessment of the rock mass permeability using the four parameters. However, it should be noted that if (1−RQD) is zero, the value of 0.01 in the term of (1−RQD) is suggested to avoid the HC-value to be zero. Currently, the study took the same weight for each factor in Equation (4). While collecting more observed data, a further study can be considered to assign a different weight for each factor to giver better correlation between the hydraulic conductivity and HC-value. The rationality of Equation (4) must be verified by observed data through in situ hydraulic tests.

2.3 Study on correlation of hydraulic conductivity and HC-system

To verify rationality of Equation (4), the study collected in situ hydraulic test data to determine a relationship between hydraulic conductivity and HC-values. The needed data include rock core logs, BHTV (Borehole Acoustic Televiewer) image logs, locations of hydraulic tests, and hydraulic conductivity results. The hydraulic test results of boreholes were used to perform the dependence of HC on hydraulic conductivity.

2.3.1 Description of study area, boreholes, BHTV investigation and hydraulic test data

The study area is located in Taiwan. Taiwan's strata are distributed in long and narrow strips, almost parallel to the island's axis. Metamorphic rock lies under the Central and Snow Mountain Ranges. Sedimentary rock forms part of the island-wide piedmonts and coastal plains as well as the Coastal Mountain Range. The island of Taiwan has three geological zones divided by longitudinal faults: the Central Range, Western Piedmont and Eastern Coastal Mountain Range zones (Figure 1).

About 26 hydraulic conductivity measurements and borehole image scanning using BHTV were conducted in four boreholes in Western Piedmont, primarily at three sites: Da-Keng, Shang-Ming, and Caoling (Figure 1) in which borehole HB-94-01 is in the Da-Keng site, boreholes HB-95-01 and HB-95-02 are in the Shang-Ming site, and borehole CH-04 is in the Caoling site. Besides, the Da-Keng and Caoling sites are in central Taiwan and the Shang-Ming site is in southern Taiwan. The dominant rock strata of the Shang-Ming site include Miocene sedimentary rock with layers of sandstone or shale or their alternation. The major structures consist of a series of parallel easterly inclined thrust faults and folds, which often form local fractured zones, including geological structures such as the Pingshi fault, the Biauhu fault, and the Chin-Shan fault. In addition, borehole HB-94-01 in the Da-Keng site and borehole CH-04 in the Caoling site also have similar rock strata but without geological structures. Based on the loggings and geological analysis, HB-95-01 and HB-95-02 are strongly influenced by the faults; nevertheless, HB-94-01 and CH-04 are not. Rock core photos (Figure 2(a)) indicated soft and cohesive gouges are extensive in borehole HB-95-02; while the borehole CH-04 is not influenced by the faults (Figure 2(b)).

The depth of the boreholeHB-94-01 is 110 m. The principal lithologic units for the borehole are sandstone and siltstone. The interval of 36 m to 44 m is a fractured zone compared to other depths in the borehole. A total of 8 hydraulic tests using a double packer system were carried out to determine hydraulic conductivity (Sinotech Engineering Consultants, LTD., 2005). The strategy of the test design from the drilling work was to determine hydraulic properties from different geological structures such as no fracture, a single fracture, or multiple fractures at different depths. The drilling depths of HB-95-01 and HB-95-02 are 250 m and 350 m, respectively. The principal lithologic units for HB-95-01 are sandstone, argillaceous sandstone, and sandy mudstone. The principal lithologic units for HB-95-02 are

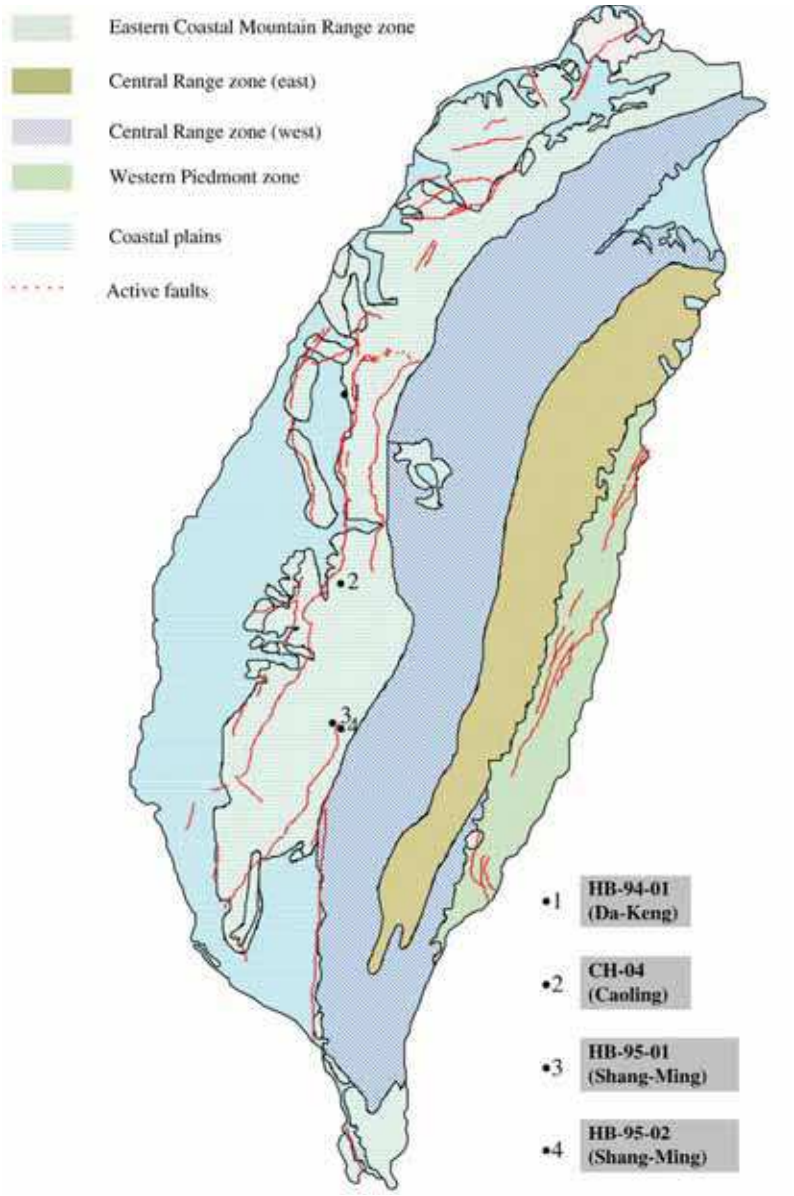

Fig. 1. Location of major faults and four boreholes for this study in Taiwan

sandstone, argillaceous sandstone, and sandstone mixed with some mudstone. HB-95-01 and HB-95-02 are close to the Biauhu fault and Pingshi fault, respectively. Rock core data indicated soft and cohesive gouges are extensive in both boreholes (Figure 2) in which the hydraulic properties of fault-related rocks can be studied. The study completed 3 and 14 hydraulic tests in HB-95-01 and HB-95-02, respectively (Sinotech Engineering Consultants,

LTD., 2007). The strategy of the test design was to determine hydraulic conductivity in more permeable zones and clay-rich gouge zones. Besides, the drilling length of borehole CH-04 is 120 m. The principal lithologic units of the borehole CH-04 are mainly sandstone, shale, and sandstone with some thin shale. Four different intervals were sealed by double packers for conducting the hydraulic tests. Those hydraulic test data were used for the model verification and it is described in Section 2.3.3.

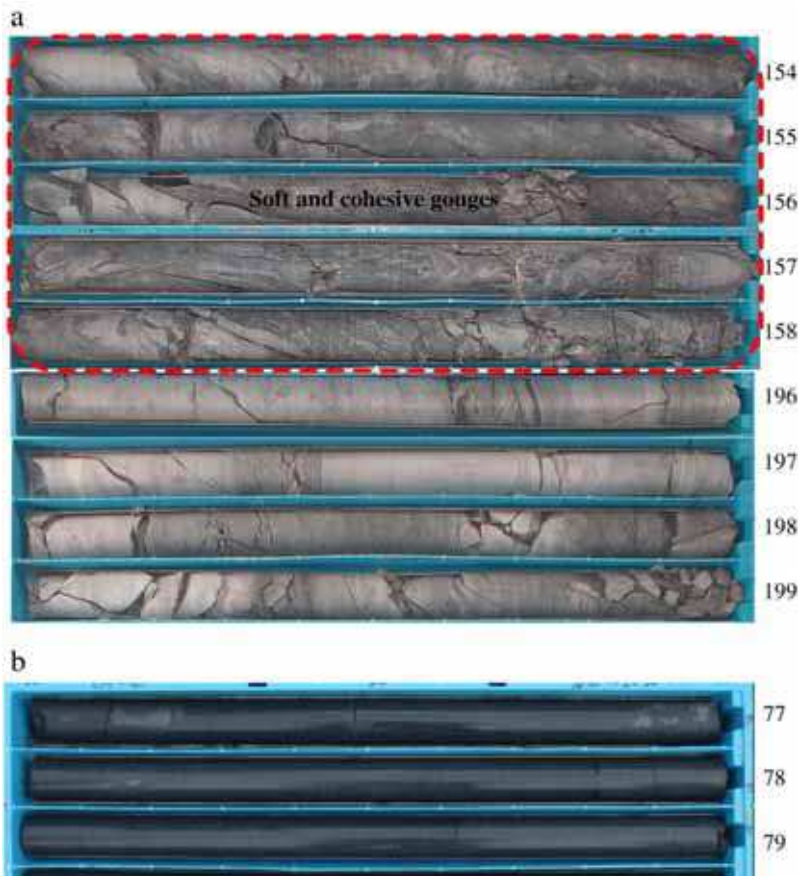

Fig. 2. (a). Rock core photos of borehole HB-95-02 with fault influence; (b). Rock core photos of borehole CH-04 without fault influence

BHTV image logs were gathered to characterize lithology, gouge and fractures for each borehole and essential to the proper design of hydraulic testing. Figure 3 shows two hydraulic test zones and corresponding BHTV images from different boreholes. It is obvious that fractures or shear band can be identified clearly using the high-resolution BHTV. The BHTV image in Figure 3(a) shows multiple fractures. This information with a double packer system (Figure 4) can be used to investigate hydraulic property of a water-bearing zone of subsurface. The BHTV image in Figure 3(b) shows shear band. This information can be utilized to investigate hydraulic property of fault-related rocks.

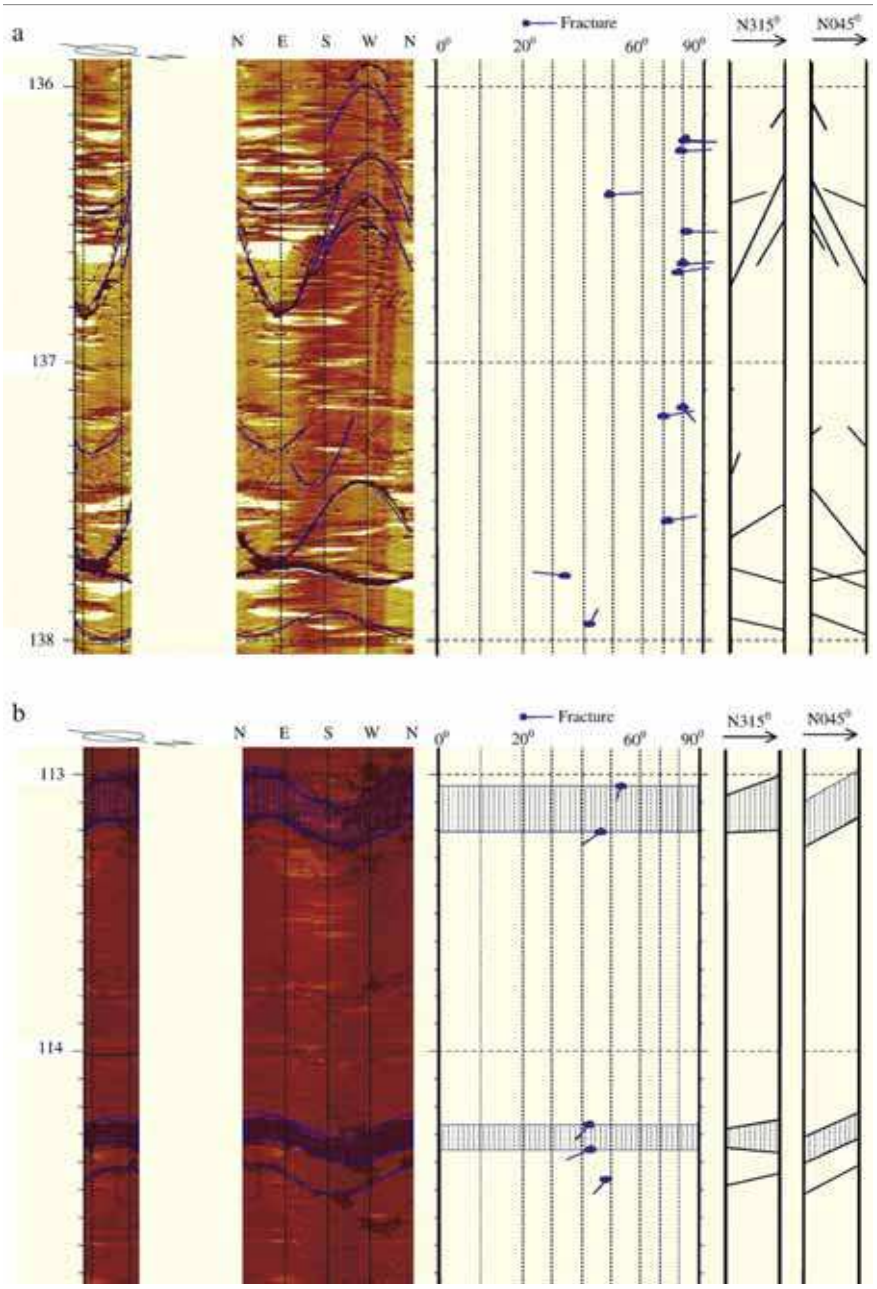

Fig. 3. (a). hydraulic test interval and corresponding BHTV image (depth 136 m-138 m, HB-95-01); (b). hydraulic test interval and corresponding BHTV image (depth 113 m-115 m, HB-95-02)

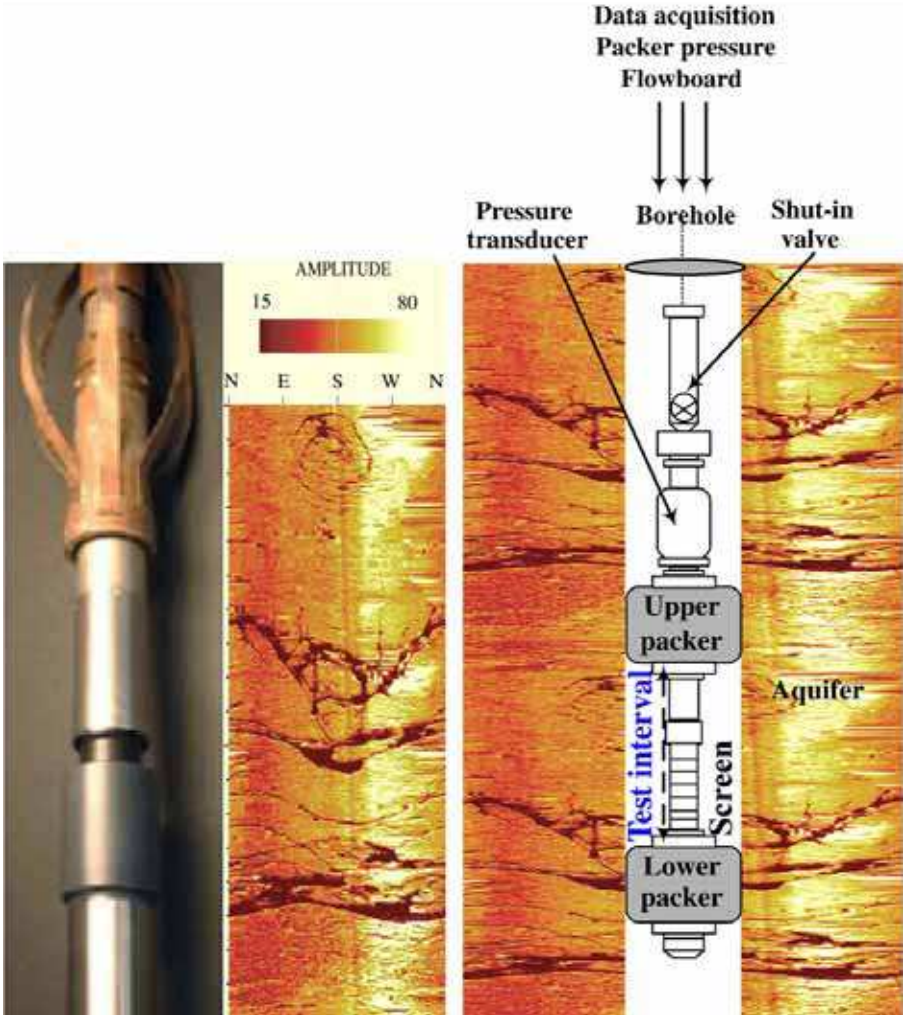

Fig. 4. Schematic drawing of BHTV, acoustic image of borehole, and double packer system

In this study, 26 hydraulic test data collected during hydraulic tests can be analyzed by analytical methods. Water pressure and discharge rate measurements with time for each hydraulic test were collected. The data analysis was performed using a professional version of the AQTESOLVE test analysis software, which enables both virtual and automatic type curve matching (Duffield, 2004). The quantitative evaluation of hydraulic parameters was carried out as an iterative process of the best-fit theoretical response curves based on the measured data of the hydraulic test. Figure 5 shows the evaluation of hydraulic parameters using AQTESOLVE. For the test interval of 118.5 m to 121.7 m, although three fractures and a fracture zone of approximately 7.25 cm thickness were seen on the borehole image, lack of interconnectivity of fractures and soft and cohesive gouges existing at the fractures may reduce the permeability of rock masses.

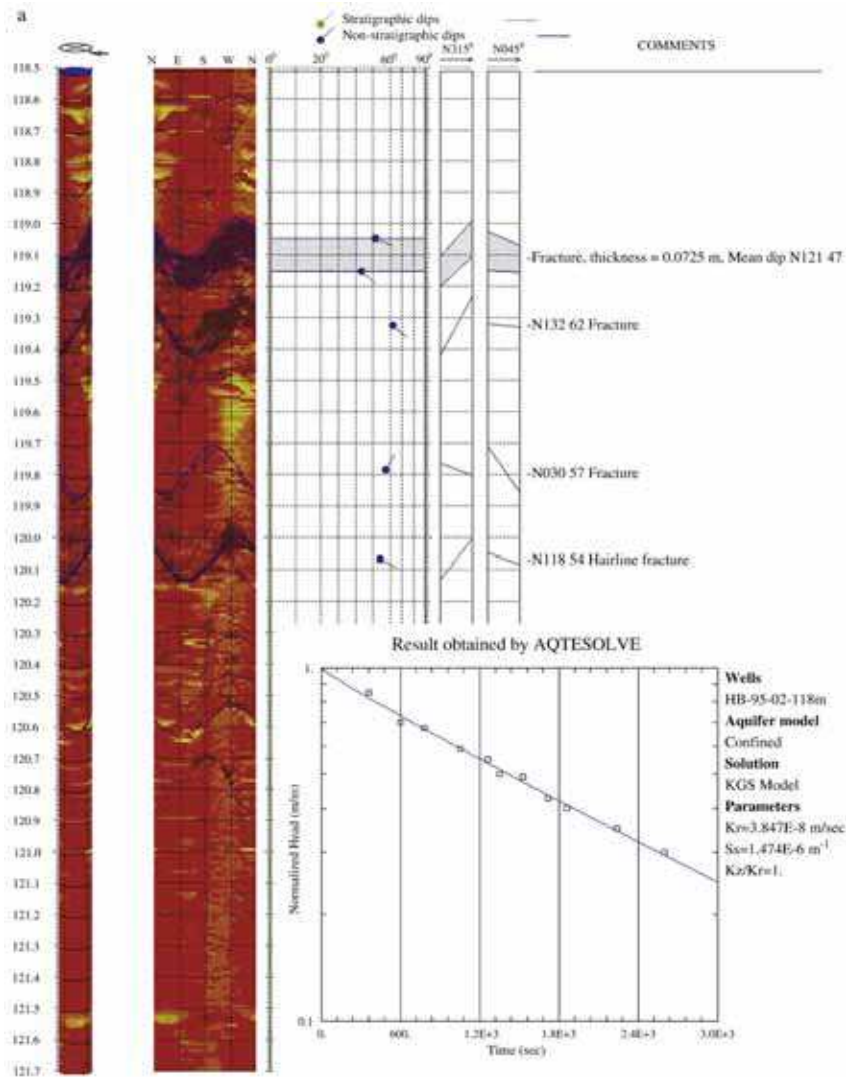

Fig. 5. Evaluation of hydraulic parameters using AQTESOLVE and BHTV images at pack-off zones of 118.5 m to 121.7 m in borehole HB-95-02

2.3.2 Relationship between hydraulic conductivity and HC-system

Regression analysis was performed to estimate the dependence of HC on hydraulic conductivity. A total of 22 hydraulic test data (borehole CH-04 data not included) were applied to the study. HC-values for the hydraulic tests can be computed from borehole image data and rock core data, in which the values of RQD and GCD at each test interval can be calculated from borehole image data and rock core data with Equations (1) and (3), respectively. The value of DI can be calculated using Equation (2). The value of LPI for each

test zone can be obtained from rock core data and Table 2. Table 3 shows the calculated results for the HC-system based on the verified data. The regression results indicated that a power law relationship exists between the hydraulic conductivity and HC values with a coefficient of determination of 0.866 as shown in Figure 6. The empirical HC model is obtained as shown in Equation 5.

$$K = 2.93 \times 10^{-6} \times (HC)^{1.380}, R^2 = 0.866 \quad (5)$$

If only HB-94-01 testing data were adopted, a better correlation with the coefficient of determination of 0.905 can be obtained as shown in Equation (6).

$$K = 2.31 \times 10^{-6} \times (HC)^{1.342}, R^2 = 0.905 \quad (6)$$

It should be noted that the values of (1−GCD) inHB-94-01 borehole are all equal to 1. The results of Equation (6) demonstrate that the empirical HC model may also be more accurate for the estimation of the rock mass hydraulic conductivity if the fractures do not contain infillings. There are a few limitations that need to be noted for the use of Equation (5). The data used to develop the equation are limited in number and in the lithologies represented. From the definition of DI, DI cannot be determined for inclined boreholes because the data collected were from vertical boreholes.

Boreholes	Test intervals (m)	1-RQD/100	DI	1-GCD	LPI	HC	K (m/s)
HB-94-01	34.7-36.3	0.094	0.677	1.000	1.000	0.0635	7.06E-08
	36.4-38.0	0.438	0.662	1.000	1.000	0.2895	1.64E-06
	56.7-58.3	0.063	0.477	1.000	0.950	0.0283	1.53E-08
	74.6-76.2	0.500	0.315	1.000	0.400	0.0629	5.30E-08
	77.2-78.8	0.010	0.291	1.000	0.400	0.0012	4.22E-10
	82.6-84.2	0.125	0.242	1.000	0.400	0.0121	2.31E-09
	90.2-91.8	0.010	0.173	1.000	0.400	0.0007	2.86E-10
	94.2-95.8	0.500	0.136	1.000	0.400	0.0273	4.53E-09
HB-95-01	99.0-101.9	0.345	0.598	0.200	0.400	0.0165	9.80E-09
	117.2-120.1	0.690	0.526	1.000	0.850	0.3081	9.76E-07
	133.2-136.1	0.724	0.461	0.286	1.000	0.0954	4.68E-08
HB-95-02	88.6-91.4	0.071	0.743	1.000	0.600	0.0318	1.56E-07
	96.0-99.2	0.031	0.721	1.000	0.600	0.0135	2.42E-08
	118.5-121.7	0.219	0.657	0.071	0.700	0.0072	1.36E-09
	134.8-138.0	0.344	0.610	0.727	0.700	0.1068	1.17E-07
	154.8-158.0	0.938	0.553	0.103	0.700	0.0376	1.99E-08
	173.0-176.2	0.938	0.501	0.103	0.700	0.0340	9.08E-09
	189.8-193.0	0.594	0.453	1.000	0.700	0.1883	1.01E-06
	196.6-199.8	0.563	0.434	0.500	1.000	0.1220	6.00E-08
	213.2-216.0	0.679	0.387	1.000	1.000	0.2625	4.54E-07
	249.0-251.8	0.393	0.285	0.091	0.700	0.0071	4.03E-09
	272.0-274.8	0.214	0.219	1.000	0.700	0.0328	3.36E-08

Table 3. The calculated results for HC-system based on 22 hydraulic test data

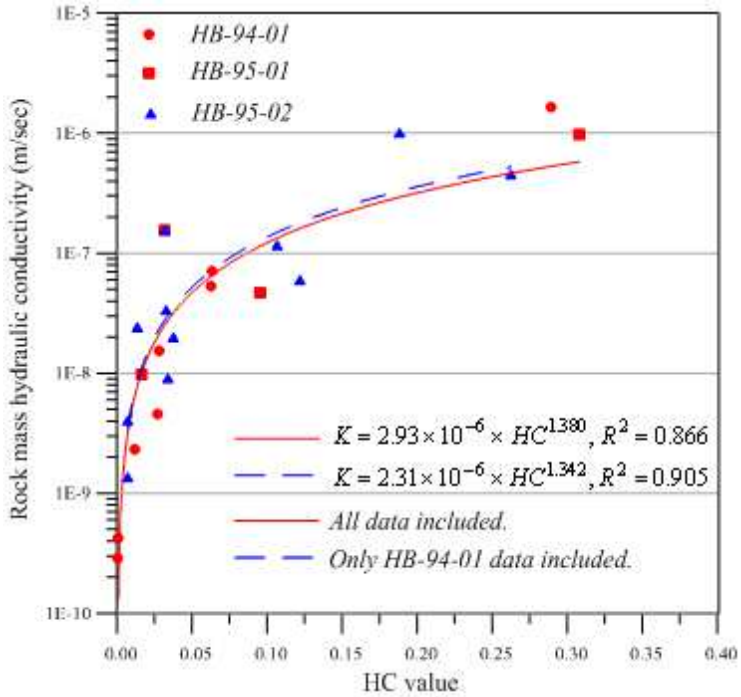

Fig. 6. Relationship between hydraulic conductivity and HC values

2.3.3 The empirical HC model verification

In order to further verify the feasibility of the proposed empirical HC model, the model verification is conducted. Borehole CH-04 data was adopted to verify the empirical HC model. The depth from 24.5 m to 26.6 m, 32.5 m to 34.1 m, 65.7 m to 67.8 m, and 77.8 m to 79.9 m were sealed by double packers for conducting the hydraulic tests. The quantitative evaluation of hydraulic parameters was then performed using AQTESOLVE. Table 4 shows four hydraulic test data for the model verification, in which $K_{HC\text{-}model}$ and $K_{in\text{-}situ}$ represent K obtained by Equation (5) and the in situ hydraulic test, respectively. Figure 7 shows that the comparison of the rock mass hydraulic conductivity obtained by in situ test and that from the estimation of the empirical HC model. Very good correlation can be found (Figure 7). This verification example demonstrates that the empirical HC model is able to determine the rock mass hydraulic conductivity for different sites in which the lithologic conditions are similar.

Test intervals (m)	RQD (%)	DI	1-GCD	LPI	HC	$K_{HC\text{-}model}$	$K_{in\text{-}situ}$
24.5-26.6	81.0	0.787	0.952	0.55	0.0785	9.06E-08	7.14E-08
32.5-34.1	43.8	0.723	0.975	0.55	0.2179	3.69E-07	1.11E-06
65.7-67.8	47.6	0.444	0.976	0.55	0.1248	1.71E-07	9.95E-08
77.8-79.9	95.2	0.343	1.000	0.55	0.0090	4.59E-09	9.09E-09

Table 3. Four hydraulic test data for the model verification

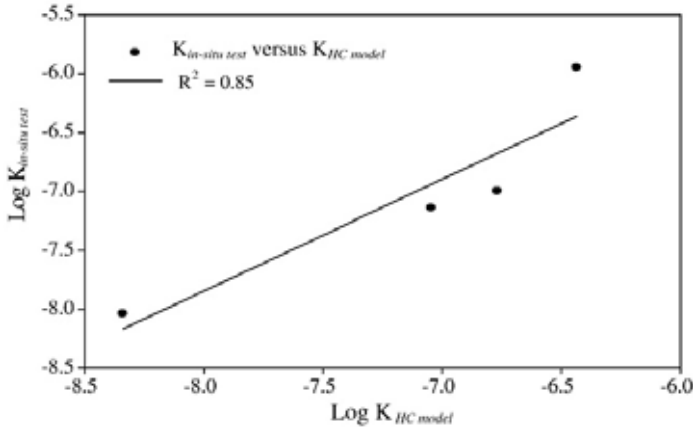

Fig. 7. Correlation between $K_{HC\text{-}model}$ and $K_{in\text{-}situ}$

2.3.4 Application of HC model

According to the above study results, the high correlation between hydraulic conductivity and HC implies that the new rock mass classification in the presented study is reasonable. It may provide two important applications in hydrogeology. The first application is that the regression equation (Equation (5) or Equation (6)) is capable of providing a useful tool to predict hydraulic conductivity of fractured rocks based on measured HC-values. By using this approach, hydraulic conductivity data in a given site can be directly acquired, which removes the cost on hydraulic testing. Secondly, for in-situ aquifer tests the HC-system is a valuable new rock mass classification system for preliminary assessment of the degree of permeability in a pack-off interval of a borehole. It is beneficial to the hydraulic test design.

3. The second empirical model

In recent years, many borehole hydrogeological investigations have been conducted to understand the relationship between hydraulic conductivity and fracture properties. For example, Tanaka and Miyakawa (1992) reported that some hydraulically conductive regions within a borehole existed in high-density fracture zone. Their results were supported by data acquired through packer tests and borehole televiewer logging. In addition, Gustafson et al., (1991) described that 44 to 61% of fractures in granite are non-conductive based on the field hydrological tests. By performing similar approaches, Hamm et al., (2007) demonstrated that the fracture aperture has stronger relationship to hydraulic conductivity than fracture frequency. They also proposed that the cubic fracture aperture model has close relationship to transmissivity with the highest correlation coefficient of 0.88.

In this study, a hydrogeologic investigation employing a series of subsurface exploration technologies was conducted at three active landslide sites in southern Taiwan. Each site was initially investigated with borehole televiewer logging to identify potentially significant fracture features and fracturing degree at depth and its hydrogeologic implications. Flowmeter logging was then performed to measure high permeability zones and fracture hydraulic connectivity along the borehole. Based on the prospecting results, test sections of hydraulic tests can be arranged. The hydraulic packer tests were carried out to further

characterize the hydrogeologic system of the site and quantitatively determine the hydraulic properties of major hydrogeologic units or different geological structures. Finally, the borehole data were used in correlation and regression analyses to define the dependence and establish models between the fracture properties and hydraulic conductivity. The rationality of the regression results was carefully assessed in predicting fractured rock hydraulic conductivity.

3.1 Investigation technologies

A comprehensive hydrogeologic investigation on slopeland may include surficial geology investigations, borehole drilling, testing of soil and rock properties from rock cores, landslide mapping with light detecting and ranging (LIDAR), resistivity image profiling (RIP), double-ring infiltration tests, borehole televiewer logging, electrical logging, flowmeter logging, and packer tests. This study focuses on describing borehole televiewer logging, flowmeter logging, and packer tests with the purpose of obtaining relationships between fracture properties and their corresponding hydraulic conductivity. The techniques are described as follows.

3.1.1 Borehole televiewer logging

Using borehole televiewers to characterize fractured-rock properties has been adopted for many years. The tool acquires continuous, 360-degree images of the borehole wall while the probe moves along the length of the borehole. The results provide relevant geological and structural information needed to hydraulically analyze the subsurface, such as the location, orientation and angle of the fractures, fracture width, infilling material of fractures, and structural planar features. In addition, the borehole image is capable of clarifying the uncertainties of the traditional rock core drilling technique, including those derived from human errors for misplacing rock core samples from its original place, or interpretation for missing intervals (Williams & Johnson, 2004; Hsu et al., 2007). Generally, borehole televiewers are of two types, including: the acoustic televiewer (ACTV) and the optical televiewer (OPTV) (Figure 8). The ACTV uses a fixed acoustic transducer and rotating acoustic mirror to scan the borehole wall with a focused ultrasound beam. The amplitude and travel time of the reflected acoustic signal are recorded simultaneously as separate image logs. The OPTV system consists a ring of lights, a hyperboloidal mirror, and video camera housing in the transparent window. The OPTV is capable of providing real-time borehole images (Williams & Johnson, 2004). Each probe has its own suitable prospecting environments that depend on specific groundwater conditions. Therefore, both acoustic and optical televiewers were used in this study.

3.1.2 Heat-pulse flowmeter logging

The heat-pulse flowmeter (HPFM) system consists of a wire-grid heating element and two sensitive thermistors (heat sensors) located above and below the wire-grid. The wire-grid generates a sheet of heat in the water and the heat migrates towards one of the thermistors, depending on direction and rate of groundwater flow (Sloto & Grazul, 1989). The direction and rate of flow can be computed once the peak temperature has been detected by the thermistor (Figure 9). When the stationary measurements are conducted at several depths along a borehole, the distribution of groundwater velocity can be obtained. This not only provides useful information to characterize the aquifer permeability, but also brings good

indications to identify the location of the flow path, water-producing/receiving zones, and fracture connectivity (Paillet, 1986; Miyakawa et al., 2000; Williams & Paillet, 2002). In addition, Miyakawa et al. (2000) pointed out that the HPFM is usually carried out by pumping water into or extracting water from the borehole, because it is difficult to detect hydraulic pathways in a natural state due to low groundwater velocities.

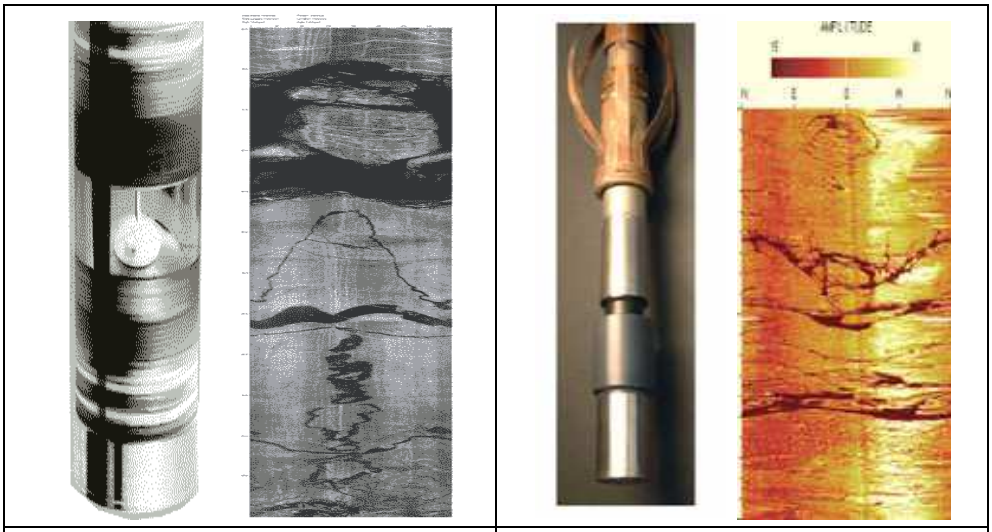

(a) Optical televiewer (b) Acoustic televiewer

Fig. 8. The televiewer and scanned borhole images

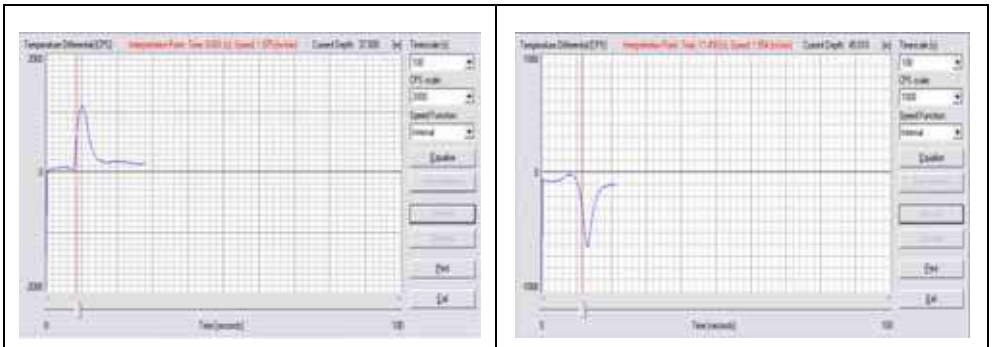

(a) The upward flow heat-pulse curve (b) The downward flow heat-pulse curve

Fig. 9. The heat-pulse curve (the elapsed time in X-axis and the temperature difference measured by the thermistor in Y-axis)

3.1.3 Double packer hydraulic test

The double packer hydraulic test is one of the most common approached applied to determining the hydraulic conductivity and storage coefficient along discrete sections of a

borehole. It is now recognized that this approach is capable of investigating the variability of a borehole as it intersects various hydrogeological units.
The double packer hydraulic test was conducted by isolating a section of borehole with a set of packers and measuring the rate of flow and/or pressure over a period of time. The system adopted in this study contained two inflatable rubber packers, a shut-in valve, flow meters, a submersible pump, and three transducers for measuring the piezometric pressure in the isolated interval and the areas above and below the packers. The rubber packers were inflated using nitrogen delivered through a polyethylene air line. The shut-in valve was used to open and close the hydraulic connection between the pipe string and the test section. The pumping or injection rate was measured at the land surface with a flow meter.
Four types of hydraulic tests can be applied to the double packer system including the pump test, injection test, slug test, and pressure pulse test. A pump test involves pumping at a constant or variable rate and measuring changes in water levels during pumping. In an injection test, fluid is injected into the test interval at a constant head. In the slug test, a known amount of water is delivered to the test interval and the changes in pressure are monitored as equilibrium conditions return. In a pressure head test, an increment of pressure is applied to the test interval and the pressure decay is monitored over time. Typically, the selection for type of test is based on the expected permeability of strata, the volume of rock to be sampled, and the availability of time and equipment. The data collected during the hydraulic test can be analyzed by analytical methods using professional software AQTESOLVE as stated in Section 2.3.1.

3.2 Case study and prospecting results

Borehole logging was conducted at three landslide sites in the south central portion of Taiwan (Figure 10). The purpose of the investigation was to determine the hydraulic properties from various geological structures, such as the degree of fracturing and hydraulic conductivity, to test hypotheses related to the causes of the landslides. The logging was conducted in six boreholes that ranged in depth from 70 to 80 m. Two boreholes from each of the following three sites were investigated: Tung-Chi (borehole FH-13 and FH-15), Bao-Long (FH-03 and FH-05), and Gi-Lu (borehole FH-21 and FH-23). The Tung-Chi and Bao-Long sites are located in Kaohsiung County, southern Taiwan. The principle lithologic units of the two sites are weathering slate with clay-rich gouges and fresh shale with thin layered sandstone, respectively. The Gi-Lu site is located in Pingtung County, southern Taiwan, where the dominated geologic unit composed of fresh slate with a minor amount of quartz and metamorphic sandstone.
The investigation first identified the position and degree of the fracturing using borehole televiewer logging. Second, the angle and width of fracture or fracture zone were calculated by adopting the post processing software. Lastly, flowmeter logging was used to determine the strata permeability and fracture connectivity. Based on the results of these preliminary logging data to determine favourable hydraulic conditions, test sections were selected for the double packer hydraulic test, and the results were used to determine the hydraulic conductivity for different geological structures (Figure 11). A total of 18 double packer hydraulic test sections were obtained in this study. Table 4 summarizes the results of the average fracture angle, fracture width, average flow velocity, hydraulic conductivity, and product of fracture width and flow velocity for each test section. These calculated data were used in correlation and regression analyses to define the dependence and establish models between the fracture properties and hydraulic conductivity.

Fig. 10. Location of three active landslide sites

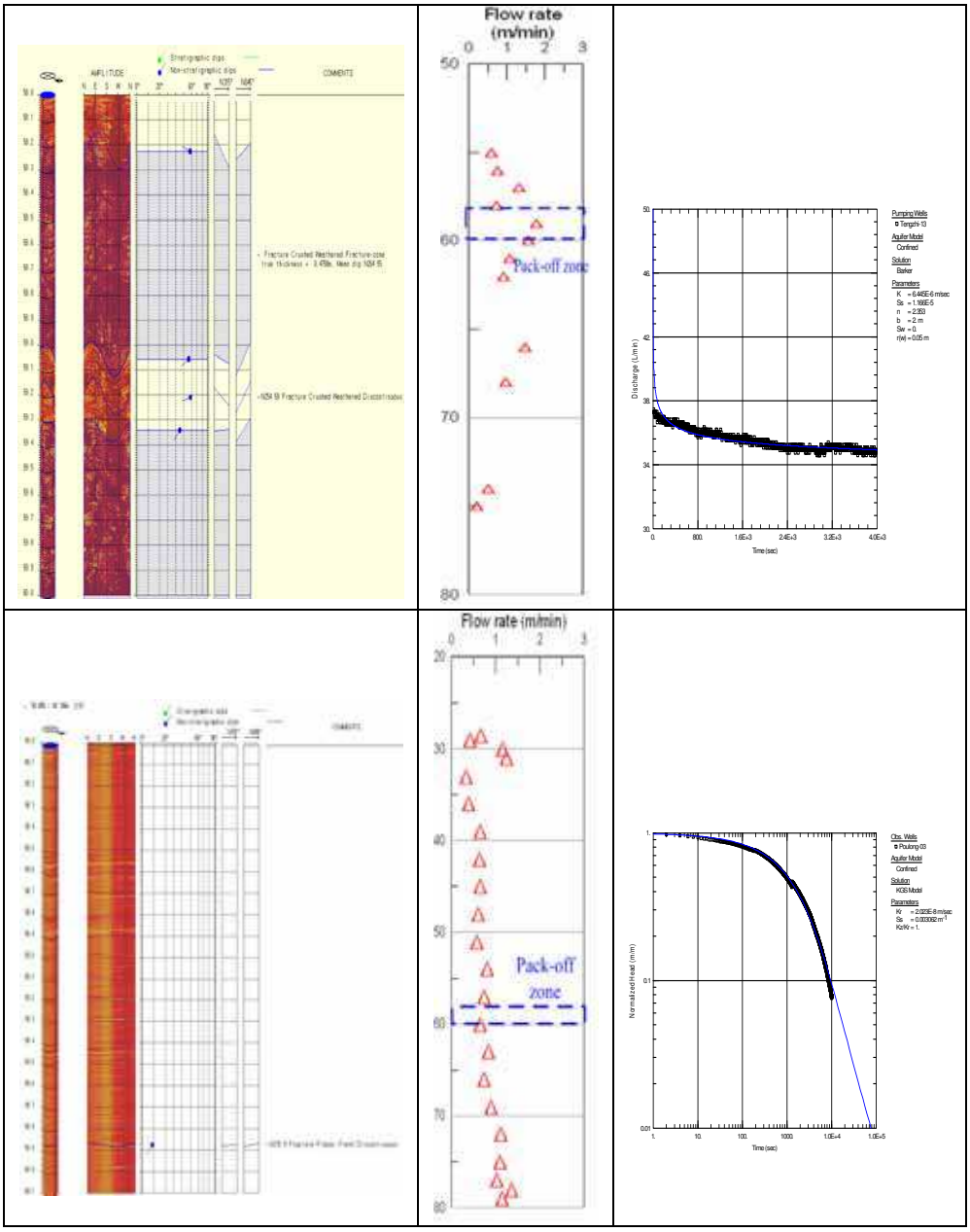

Fig. 11. The computed angle and width for single fracture or fracture zone, the measured groundwater velocity and hydraulic conductivity obtained from AQTESOLVE (from left to right) at 58.0-60.0m pack-off zones in Tung-Chi landslide site (above); and at 58.0-60.1m pack-off zones in Bao-Long landslide site (below)

Borehole	Test Intervals (m)	Average Fracture Angle, FA (deg)	Fracture (zone) Width, FW (m)	Average Flow Velocity, V (m/min)	Hydraulic Conductivity, K (m/sec)	Product of Fracture Width and Flow Velocity (FW×V)
FH-13	46.5-48.5	42.0	2.000	NA	3.59E-06	NA
	58.0-60.0	57.0	1.485	1.25	6.45E-06	1.856
	61.0-63.0	35.0	0.845	1.01	9.57E-06	0.845
	68.0-70.0	32.6	0.015	0.96	3.25E-07	0.014
FH-15	45.5-47.5	29.5	1.430	2.40	1.59E-05	3.432
	56.6-58.6	29.0	2.000	2.47	2.91E-05	4.940
	65.8-67.8	32.3	0.080	2.45	1.67E-06	0.196
FH-03	29.5-31.6	19.0	0.005	1.20	1.13E-08	0.006
	39.0-41.1	11.0	0.005	0.97	1.98E-10	0.005
	58.0-60.1	09.0	0.005	0.70	3.20E-09	0.004
FH-05	34.0-36.1	38.0	0.055	0.52	1.68E-07	0.029
	50.0-52.1	31.2	0.035	1.15	4.10E-07	0.040
FH-21	31.9-33.4	34.0	0.445	NA	8.40E-06	NA
	35.3-37.0	41.7	0.220	NA	2.54E-06	NA
	51.8-53.3	38.0	0.430	0.10	3.19E-07	0.043
	63.8-65.3	40.0	0.525	0.49	4.88E-07	0.257
FH-23	50.5-52.0	54.3	0.130	0.10	2.67E-08	0.013
	57.0-58.5	38.2	0.105	0.33	1.12E-07	0.035

NA: Non-detectable when test section above groundwater table

Table 4. The prospecting results

3.3 Data analysis

3.3.1 Correlation analysis

To define the dependence between the rock mass hydraulic conductivity and fracture angle, fracture width, and the flow velocity, a univariate correlation analysis was performed. The correlation coefficient between the different values can be computed by following equation:

$$r_{xy} = \frac{\sum_{i=1}^{n}(x_i - \bar{x})(y_i - \bar{y})}{S_x S_y} \tag{7}$$

where $\bar{x}$ and $\bar{y}$ are the sample means of x and y, S_x and S_y are the sample deviations of x and y, which are defined as:

$$S_x = \sqrt{\frac{\sum_{i=1}^{n}(x_i - \bar{x})}{n}} \tag{8}$$

$$S_y = \sqrt{\frac{\sum_{i=1}^{n}(y_i - \bar{y})}{n}} \tag{9}$$

The results of the correlation analysis are shown in Table 5. The table shows that the fracture width and flow velocity have a good correlation with hydraulic conductivity, with correlation coefficient of 0.75 and 0.69, respectively. In addition, the analysis indicates that the fracture angle and hydraulic conductivity were independent. Most noticeably, by multiplying fracture width and flow velocity, the products of two values shown strong positive correlation to hydraulic conductivity with correlation coefficient of 0.93. Since the borehole flow velocity is usually related to fracture connectivity, a strong correlation to hydraulic conductivity can be found when considering for both fractures width and connectivity.

	Correlation Coefficient			
	Average Fracture Angle, FA (deg)	Fracture (zone) Width, FW (m)	Average Flow Velocity, V (m/min)	Product of Fracture Width and Flow Velocity (FW×V)
Hydraulic Conductivity, K (m/sec)	-0.01	0.75	0.69	0.93

Table 5. The results of correlation analysis

3.3.2 Regression analysis

A regression analysis was used to establish the relationship between hydraulic conductivity and fracture angle, fracture width, flow velocity and the product of fracture width and flow velocity. Although the fracture angle and flow velocity were difficult to establish good relationship with hydraulic conductivity as shown in Table 6, a power low relationship exists between the hydraulic conductivity and fracture width in the semi-log scale with a coefficient of determination of 0.73. Furthermore, a better regression result, which the coefficient of determination of 0.83 was established between hydraulic conductivity and the product of fracture width and flow velocity in log-log scale (Figure 12) Therefore, it can be concluded that the rock mass hydraulic conductivity not only related to the fracture width, but also possesses strong relationship when their corresponding connectivity took into account. This regression results is desired to predict hydraulic conductivity of the study area based on borehole televiewer and flowmeter logging results, which removes cost of packer test for additional test intervals or boreholes.

Factors Related to Hydraulic Conductivity	Best Regression Equation	Coefficient of Determination (R^2)
Average Fracture Angle, FA (deg)	$K = 1.79E\text{-}13(FA)^{4.27}$	0.42
Fracture (zone) Width, FW (m)	$K = 5.42E\text{-}6(FW)^{1.30}$	0.73
Average Flow Velocity, V (m/min)	$K = 2.65E\text{-}8\exp(2.18V)$	0.28
Product of Fracture Width and Flow Velocity (FW×V)	$K = 6.29E\text{-}6(FW\times V)^{1.25}$	0.83

Table 6. The results of regression analysis

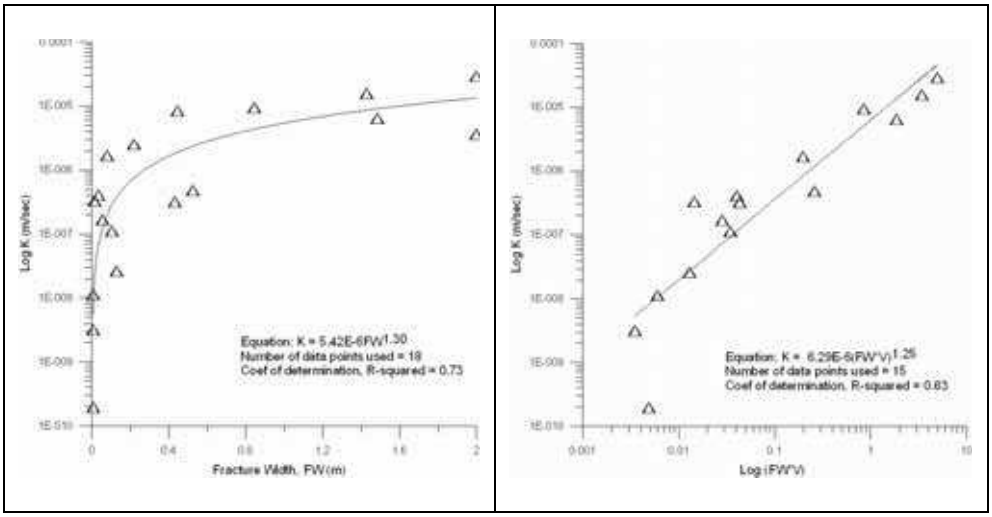

Fig. 12. Regression results of Fracture width (FW) with hydraulic conductivity (left); and the product of fracture width and flow velocity (FW×V) with hydraulic conductivity (right).

3.3.3 Model verification

In order to further verify the applicability of the regression result, the verification was conducted using another two in-situ borehole prospecting data obtained in a nuclear power plant. The geologic unit of the site is mainly composed of shale or shale with thin layered sandstone. Both televiewer and flowmeter loggings were performed, and five intervals were selected for packer test. The quantitative evaluation of hydraulic conductivity was then applied using AQTESOLV based on the data of packer test. Table 7 shows five test data for the model verification, in which K_{FW} and $K_{FW\times V}$ represent K obtained by corresponding equations in Table 6; $K_{in\text{-}situ}$ represents K obtained by the in situ hydraulic test. Figure 13 shows the comparison of rock mass hydraulic conductivity obtained from in-situ test data and from regression results. The coefficient of determination between in-situ hydraulic

Borehole	Test Intervals (m)	Fracture (zone) Width, FW (m)	Average Flow Velocity, V (m/min)	Product of Fracture Width and Flow Velocity (FW×V)	Predicted Hydraulic Conductivity, K_{FW}(m/sec)	Predicted Hydraulic Conductivity, $K_{FW\times V}$(m/sec)	Measured Hydraulic conductivity, $K_{in\text{-}situ}$ (m/sec)
BH-37	65.5-67.0	0.08	2.99	0.24	2.03E-07	1.05E-06	1.17E-06
	73.5-75.0	0.07	2.22	0.14	1.55E-07	5.59E-07	2.31E-07
BH-43	28.0-29.5	0.17	3.22	0.55	5.41E-07	2.96E-06	1.16E-05
	43.0-44.5	0.08	2.24	0.18	2.03E-07	7.33E-07	2.10E-07
	54.0-55.5	2.00	2.60	5.20	1.33E-05	4.94E-05	1.81E-05

Table 7. Five test data for model verification

conductivity and that predicted from the product of fracture width and velocity is 0.74, which is higher than the hydraulic conductivity predicted from fracture width only. Although the prediction still possesses some deviations when compared to real data (a predicted value is an order of magnitude lower than the measured value), the verification result demonstrated that the regression equation is capable of estimating the fractured rock hydraulic conductivity without packer testing, especially for the site with similar lithologic environments.

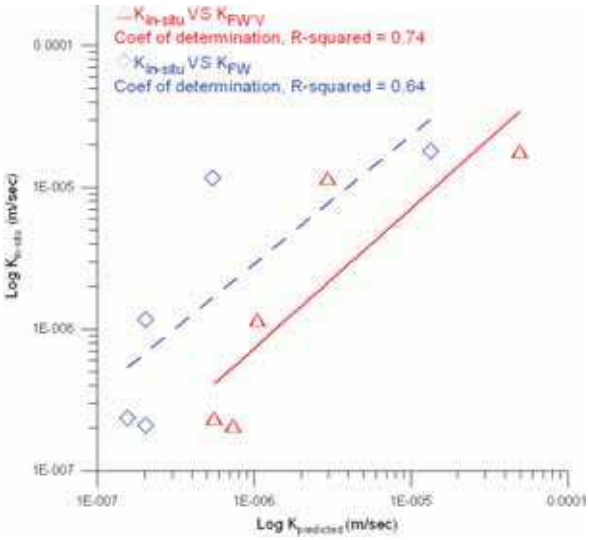

Fig. 13. Verification of regression results: hydraulic conductivity predicted from the product of fracture width and flow velocity (solid line); hydraulic conductivity predicted from fracture width only (dash line)

4. Conclusions

The estimation of rock mass hydraulic conductivity using feasible empirical equations possesses great advantages. This chapter proposes two empirical models to estimate hydraulic conductivity of fractured rock mass with the features of high efficiency and low cost.

The first empirical model was based on the rock mass classification concept. The study develops a new rock mass classification scheme for estimating hydraulic conductivity of fractured rocks. The new rock mass classification system called as "HC-system" based on the following four parameters: rock quality designation (RQD), depth index (DI), gouge content designation (GCD), and lithology permeability index (LPI). HC-values can be calculated from borehole image data and rock core data. To verify rationality of the defined HC-system, the study collected data from the results of two hydrogeological investigation programs in three boreholes with 22 in-situ hydraulic tests to determine a relationship between hydraulic conductivity and HC. Regression analysis was performed to estimate the dependence of HC on hydraulic conductivity. The field results indicated that the rock mass in the study area has the conductivity between the order 10^{-10} and 10^{-6} m/s at the depth

between 34 m and 275 m below ground surface. The regression results demonstrated that a power law relationship exists between the two variables with a coefficient of determination of 0.866. Besides, the model verification using another borehole data with four additional in-situ hydraulic tests was also conducted to further verify the feasibility of the proposed empirical HC model. The regression equation provides a useful tool to predict hydraulic conductivity of fractured rocks based on measured HC-values. By using this regression equation, hydraulic conductivity data in a given site can be directly acquired, which removes the cost on hydraulic tests. For in-situ aquifer tests, the HC-system is a valuable new rock mass classification system for preliminary assessment of the degree of permeability in a packed-off interval of a borehole.

The second empirical model was simply based on the results of borehole televiewer logging, flowmeter logging and packer hydraulic tests at three active landslide sites in southern Taiwan. Three borehole prospecting techniques for hydrogeologic investigation of fractured rock mass were performed to explore various hydrogeologic characteristics, such as fracture width, fracture angle, flow velocity and hydraulic conductivity. By adopting a correlation analysis, the dependence between hydraulic conductivity and other prospecting data was identified. While the analysis revealed that the fracture width and flow velocity showed good correlation with hydraulic conductivity, the fracture angle and hydraulic conductivity were uncorrelated. In addition, by multiplying fracture width and flow velocity, the product of two values strongly correlated to hydraulic conductivity with the correlation coefficient of 0.93. The regression analysis also indicated that a power law relationship with a coefficient of determination of 0.83 existed between the hydraulic conductivity and the product of fracture width and flow velocity. Furthermore, the regression equation was verified using other borehole prospecting data. The results demonstrated that the regression equation is capable of predicting the hydraulic conductivity of fractured rock based on borehole televiewer and flowmeter logging results at the site with similar lithologic conditions. The study also demonstrated that such an approach is very constructive for a subsurface hydrogeologic assessment, particularly in the absence of packer test data due to a limited budget.

5. References

Barton, N.; Lien, R. & Lunde, J. (1974). Engineering classification of rock masses for the design of tunnel support, *Rock Mech.*, Vol. 6, 183-236.

Bear, J. (1972). *Dynamics of Fluids in Porous Media*, American Elsevier Publication Co., New York.

Bieniawski, Z. T. (1973). Engineering classification of jointed rock masses, *Trans. S. Afr. Inst. Civ. Eng.*, Vol. 15, 335-344.

Bieniawski, Z. T. (1989). *Engineering Rock Mass Classifications-A Complete Mannual for Engineers and Geologists in Minging, Civil, and Petroleum Engineering*, John Wiley & Sons, New York.

Black, J. H. (1987). Flow and flow mechanisms in crystalline rock, in Fluid Flow in Sedimentary Basins and Aquifers, *Geol. Soc. Special Publication No. 34*, pp. 186-200.

Burgess, A. (1977). *Groundwater Movements Around a Repository - Regional Groundwater Analysis*, Kaernbraenslesaekerhet, Stockholm, Sweden.

Carlsson, A. & Olsson, T. (1977). *Hydraulic properties of Swedish crystalline rocks-hydraulic conductivity and its relation to depth*, Bulletin of the Geological Institute, University of Uppsala, 71–84.

Deere, D. U.; Hendron, A. J.; Patton, F. D. & Cording, E. J. (1967). Design of surface and near surface construction in rock, *Proceedings of 8th U.S. Symposium. Rock Mechanics. AIME*, pp. 237-302, New York.

Duffield, G. M. (2004). *AQTESOLVE Version 4 User's Guide*, Developer of AQTESOLV HydroDOLVE, Inc., Reston, VA, USA.

Foyo, A.; Sa'nchez, M. A.; & Tomillo, C. (2005). A proposal for secondary permeability index obtained from water pressure test in dam foundations, *J Geo. Eng.*, Vol. 77, 69-82.

Gates, W .C. B. (1997). The hydro-potential(HP) value: a rock classification technique for evaluation of the ground-water potential in fractured bedrock, *Environmental & Engineering Geoscience*, Vol. 3, No. 2, 251-267.

Gustafson, G.; Rhen, I. & Stanfor, R. (1991). *Evaluation and conceptual modeling based on the pre-investigations 1986-1990*, Aspo Hard Rock Laboratory Technical Report 91-22, Swedish Nuclear and Waste Management.

Hamm, S.; Kim, M.; Cheong, J.; Kim, J.; Son, M. & Kim, T. (2007). Relationship between hydraulic conductivity and fracture properties estimated from packer tests and borehole data in a fractured granite, *Engineering Geology*, 92, 73-87.

Hsu, S.; Chung, M.; Ku, C.; Tan, C. & Weng, W. (2007). An application of acoustic televiewer and double packer system to the study of the hydraulic properties of fractured rocks, 60th Canadian Geotechnical Conference & 8th joint CGS/IAH-CNC Groundwater Conference, pp. 415-422, V1, Ottawa, Canada.

Lauffer, H. (1958). Gebirgsklassifizierung für den stollenbau, *Geo. Bauwesen*, Vol. 74, 46-51.

Lee, C. H. & Farmer, I. (1993). *Fluid flow in discontinuous rocks*, Chapman&Hall, London, UK.

Louis, C., (1974). *Rock Hydraulics in Rock Mechanics (ed. L. Muller)*, Springer Verlag, Vienna.

Miyakawa, K.; Tanaka, K.; Hirata, Y. & Kanauchi, M. (2000). Detecting of hydraulic pathways in fractured rock masses and estimation of conductivity by a newly developed TV equipped flowmeter, *Engineering Geology*, Vol. 56, 19-27.

National Research Council. (1996). *Rock fractures and fluid flow: contemporary understanding and applications*, National Academy Press, Washington DC, USA.

Paillet, F. L. & Hess, A. E. (1986). *Geophysical well-log analysis of fractured crystalline rocks at east Bull Lake*, Ontario, Canada: U.S. Geological Survey Water Resources Investigations Report 86-4052.

Sahimi, M. (1995). Flow and transport in porous media and fractured rock, Wiley-VCH.

Singhal, B. B. S. & Gupta, R.P. (1999). *Applied hydrogeology of fractured rocks*, Kluwer Academic Publishers, The Netherlands, 400 p.

Sinotech Engineering Consultants, LTD. (2005). "Tseng-Wen transbasin diversion tunnel project-supplemental geology investigation," Southern Water Resources Office, Water Resources Agency, Ministry of Economic Affairs, Taiwan.

Sloto, R. A. & Grazul, K. E. (1989). *Results of borehole geophysical logging and hydraulic tests conducted in area D supply wells, former U.S. Naval Air Warfare Center; Warminster, Pennsylvania*, Water Resource Investigation Report 01-4263, U.S. Geological Survey.

Snow, D. T. (1969). Anisotropic permeability of fractured media, *Water Resources Research*, Vol. 5, No. 6, 1273-1289.

Spitz, K., and Moreno, J. (1996). "A practical guide to groundwater and solute transport modeling," John Wiley, New York, 480 p.

Tanaka, K. & Miyakawa, K. (1992). Application of borehole television system to deep underground survey, *Jpn. Soc. Eng. Geol.*, Vol. 32, 289-303.

Terzaghi, K. (1946). *Rock defects and loads on tunnel support*, Rock Tunneling with steel supports, ed. R. V. Proctor and T. White, Commercial Shearing Co., Youngstown, OH, 15-99.

Wickham, G.E., Tiedemann, H.R., and Skinner, E.H. (1972). "Support determineation based on geologic predictions," Proc. Rapid Excav. Tunnelinf Conference, AIME, New Yprk: 43-64.

Hess, A.E. (1986). "Identifying hydraulically conductive fractures with a slow velocity borehole flowmeter." Canadian Geotechnical Journal 23: 69-78.

Sloto, R.A. and Grazul, K.E. (1989). "Results of borehole geophysical logging and hydraulic tests conducted in area D supply wells, former U.S. Naval Air Warfare Center; Warminster, Pennsylvania" Water Resource Investigation Report 01-4263, U.S. Geological Survey.

Tanaka, K. and Miyakawa, K. (1992). "Application of borehole television system to deep underground survey." Jpn. Soc. Eng. Geol. 32: 289-303.

Wei, Z. Q.; Egger, P. & Descoeudres, F. (1995). Permeability predictions for jointed rock masses, *International Journal of Rock Mechanics, Mineral Science and Geomechanics*, Vol. 32, 251-26l.

Wickham, G. E.; Tiedemann, H. R. & Skinner, E. H. (1972). Support determination based on geologic predictions, Proc. *Rapid Excavation Tunnel*, AIME, pp. 43-64, New York.

Williams, J. H. & Paillet, F. L. (2002). Using flowmeter pulse to define hydraulic connections in the subsurface: a fractured shale example, *Journal of Hydrology*, Vol. 265, 100-117.

Williams, J. H. & Johnson, C. D. (2004). Acoustic and optical borehole-wall imaging for fractured-rock aquifer studies, *Journal of Applied Geophysics*, Vol. 55, 151-159.

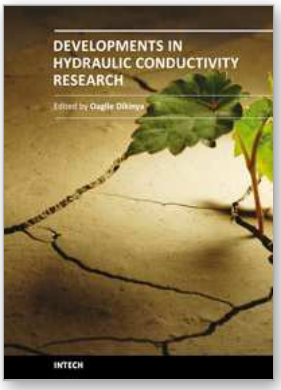

Developments in Hydraulic Conductivity Research

Edited by Dr. Oagile Dikinya

ISBN 978-953-307-470-2
Hard cover, 270 pages
Publisher InTech
Published online 28, February, 2011
Published in print edition February, 2011

This book provides the state of the art of the investigation and the in-depth analysis of hydraulic conductivity from the theoretical to semi-empirical models perspective as well as policy development associated with management of land resources emanating from drainage-problem soils. A group of international experts contributed to the development of this book. It is envisaged that this thought provoking book will excite and appeal to academics, engineers, researchers and University students who seek to explore the breadth and in-depth knowledge about hydraulic conductivity. Investigation into hydraulic conductivity is important to the understanding of the movement of solutes and water in the terrestrial environment. Transport of these fluids has various implications on the ecology and quality of environment and subsequently sustenance of livelihoods of the increasing world population. In particular, water flow in the vadose zone is of fundamental importance to geoscientists, soil scientists, hydrogeologists and hydrologists and allied professionals.

InTech Europe
University Campus STeP Ri
Slavka Krautzeka 83/A
51000 Rijeka, Croatia
Phone: +385 (51) 770 447
Fax: +385 (51) 686 166
www.intechopen.com

InTech China
Unit 405, Office Block, Hotel Equatorial Shanghai
No.65, Yan An Road (West), Shanghai, 200040, China
中国上海市延安西路65号上海国际贵都大饭店办公楼405单元
Phone: +86-21-62489820
Fax: +86-21-62489821